

Electronic spectrum of aperiodic ladder networks with side coupled quantum dots

Biplab Pal* and Arunava Chakrabarti†

Department of Physics, University of Kalyani, Kalyani, West Bengal-741 235, India

The energy spectra of quasi-one dimensional aperiodic ladder networks are analyzed within a tight binding description. In particular, we show that if a selected set of sites of each strand of a general n -arm ladder are side-coupled to quantum dots, absolutely continuous subbands can be generated in the spectrum if one tunes the dot-strand coupling appropriately. Typical cases with two and three strand Fibonacci ladders are discussed in details, and the possibility of re-entrant insulator-metal transition is discussed as one increases the number of strands. Our results are analytically exact.

PACS numbers: 71.30.+h, 72.15.Rn, 03.75.-b

I. INTRODUCTION

Anderson localization [1–3] of electronic states in a disordered system is a path breaking observation that has extended its realm well beyond the electronic properties of disordered solid materials, and has been found out to be ubiquitous in a wide variety of systems such as the photonic [4, 5], phononic [6, 7], polaronic [8, 9], or plasmonic lattices [10, 11] to name a few. Artificial, tailor made geometries developed using the improved fabrication and lithographic techniques have been instrumental in testing the validity of the basic theory of exciton localization in presence of disorder, which includes the direct observation of localization of matter waves in recent times [12–14].

Localization is a result of quantum interference that has the strongest manifestation in one dimension where all the single particle states exhibit an exponential decay of amplitude as one moves away from a particular lattice point. For dimensions beyond one, the states retain their characteristic decay in amplitude, with the addition of a possibility of a metal-insulator transition in three dimensions. The results have been substantiated by calculations of the localization length [15, 16], density of states [17] and their multi-fractality [18, 19].

Extensive work has also revealed the intricacies of the single parameter scaling hypothesis [3], its validity [20] or, variance [21], and even violation [22, 23] in low dimensional systems within a tight binding approximation. The studies have subsequently been consolidated by direct experimental measurements of conductance distribution in quasi-one dimensional gold wires [24].

In the last couple of decades variations in the canonical cases of Anderson localization have surfaced, particularly, within a tight binding description. Resonant tunneling of electronic states has been shown to arise even in a one dimensional disordered system as a consequence of certain special kinds of positional correlation [25–28]. Discrete energy levels corresponding to *extended eigen-*

functions [25], appear within a typical point spectrum exhibited by the randomly disordered lattices rendering the two-terminal transport completely ballistic at special values of the Fermi level. Even a spectral continuum and metal-insulator transition [26–28] in one, or quasi-one dimensional systems turns out to be quite a possibility.

In this context, an engineering of extended states in an otherwise disordered system turns out to be quite meaningful, and challenging. The local positional correlations in disordered [25] or quasi-periodic systems [29] generate isolated extended states, and existence of real continuous bands are reported only recently in quasi one dimensional or two dimensional systems with diagonal disorder [27, 28].

In this communication we show that, in quasi-one dimensional ladder networks with off-diagonal quasi-periodicity (or even disorder) it is possible to generate absolutely continuous bands of energy eigenvalues. Ladder networks within the framework of tight binding model have already been exploited to gain insight into charge transport in DNA [30]. The ladder models also provide interesting physics related to ladder polymer structures and poyacene lattice topology [31, 32]. Comparatively speaking, engineering absolutely continuous portions in the energy spectrum of the ladder networks, disordered or quasi-periodic, still remains to be explored to open up any new physics, or to gauge the possibility of devising novel low dimensional filter networks. Though, there have been recent steps taken in this direction [27, 28], the work necessarily concentrated on diagonal disordered models within a tight binding framework, and to the best of our knowledge the case of off-diagonal disorder remains unaddressed. Interestingly, we observe that, generating absolutely continuous subbands in the electronic spectrum of such quasi-1-d systems, we need to attach quantum dot (QD) or a cluster of dots from one side to a selected set of lattice points only. We discuss the results explicitly in terms of quasi-periodic two and three arm ladder network models using a tight binding Hamiltonian and a decimation renormalization method. The highlight of the work is to unravel the possibility of a *critical to extended state* crossover in case of the quasi-periodic ladder network (QPLN), particularly when the number of arms ‘ n ’ in the transverse direction increases. The parallel for

*Electronic address: biplabpal@klyuniv.ac.in

†Electronic address: arunava_chakrabarti@yahoo.co.in

the randomly disordered model will be again a metal-insulator transition, but now in the purely off-diagonally disordered situation. This is to be contrasted with the earlier studies [27, 28] that were made exclusively with diagonal disorder.

The system is described by a tight binding Hamiltonian. The on-site potential at every lattice point is kept constant, while the nearest neighbor hopping integral along the arms of the ladder assumes two values dictated by the growth rule of the desired quasi-periodic sequence. The electron can tunnel between the arms of the ladder by hopping from one site to its corresponding site on the other arm through the *tunnel hopping integral* (THI) ξ (see Fig. 1). The sites marked by α in each arm of the ladder is coupled to a single level QD [33] attached from one side. The QD is coupled to the α -site via a hopping integral λ . There is no positional correlation, short range or long range in the conventional sense [25, 26]. Attachment of QD's from a side can quench the conductance of a linear chain [34], but an array of QD in a ladder can have reverse effect, as will be seen.

We show that, for a particular relationship between the nearest neighbor hopping integrals along the ladder arm and λ , and for a special value of QD potential, we get *absolutely continuous subbands* in the spectrum. This immediately raises a non-trivial issue that, the nature of the electronic spectrum and the eigenstates can become sensitive to the *numerical values* of the Hamiltonian parameters – a fact that is not observed in the conventional Anderson localization problem. Conventional *critical eigenstates* can, in principle, superpose on such continuous subbands, giving rise to the possibility of a *phase transition* (when the system grows in the transverse direction), or at least a crossover between the *critical states* and the extended *Bolch-like* ones. The corresponding two-terminal transmission will exhibit a transition from being very low (for the critical state regime) to unity (for the extended subband regime). Our results are analytically exact.

In section II we describe the Hamiltonian and the basic working principle for the two and three strand quasi-periodic ladders constructed following a Fibonacci sequence, and the real space renormalization scheme to obtain the energy spectrum and to judge the character of the single particle states. The two terminal transport is discussed in section III, and in section IV we draw our conclusion.

II. THE MODEL AND THE METHOD

To describe the system we use a tight-binding framework. In Wannier basis the Hamiltonian of the ladder network consisting of a finite, but arbitrarily large number of strands n reads,

$$H = \sum_i \epsilon_i c_i^\dagger c_i + \sum_{\langle ij \rangle} t_{ij} [c_i^\dagger c_j + h.c.] \quad (1)$$

where, ϵ_i is in general $n \times n$ on-site potential matrix at the i -th vertical rung, whose explicit forms will be given below for the two-strand and three-strand ladders. We shall discuss the results for two and three strand ladders only. Generalization to an n -strand ladder is trivial. $c_i^\dagger(c_i)$ is the creation (annihilation) operator, represented by rows (columns) of appropriate dimension, and t_{ij} is the $n \times n$ hopping matrix representing hopping along and in between strands of the ladder, n being equal to 2, 3 or any integer.

The Fibonacci ladder network is grown following the binary Fibonacci sequence of two letters L and S (representing two bonds) along the horizontal direction. The growth rule is, $L \rightarrow LS$ and $S \rightarrow L$, and the sequence begins with L . The on-site potentials in each strand are designated by three symbols viz., ϵ_α , ϵ_β and ϵ_γ for sites flanked by two L -bonds, L on left and S on right, and L on right and S on left respectively. The attached QD is shown as “ μ ” in Fig. 1, and The potential at the side coupled QD is designated by ϵ_D . The nearest neighbor hopping integral $t_{ij} = t_L$ or t_S along ladder-arms following the Fibonacci sequence. $t_{ij} = \xi$ is the inter-arm hopping, and $t_{ij} = \lambda$ designates the tunnel hopping between the QD and the α -sites of the ladder network. In our work, we shall assume $\epsilon_\alpha = \epsilon_\beta = \epsilon_\gamma = \epsilon_0$, $t_L \neq t_S$ and $\epsilon_D = \epsilon_\mu$. So, this is purely a *bond model* [35] as one looks at any one strand of the network. An equivalent case will be that of an *off diagonal disorder* if one speaks of a randomly disordered ladder network.

We shall analyze the problem first using a method described earlier [27, 28] in which an ‘ n ’-strand ladder is decoupled, in a new basis, into a system of n independent linear chains. The complete spectrum of the quasi 1-d system of n strands is then obtained by convolving the spectra of the individual linear chains. We illustrate the process by considering two explicit cases of two and three strand ladders. In the former case, we perform a real space renormalization group (RSRG) analysis which yields a consistent density of states spectrum that is in conformity with our results obtained earlier. The two terminal transmission spectrum is also computed using the RSRG decimation scheme to highlight the effect of the side coupled QD's.

The analysis will be carried over to the three strand ladder, and a generalization to the n strand case will be discussed using arguments.

A. The two-strand Fibonacci ladder

1. The decoupling of the strands and the spectral analysis

To begin with we renormalize the potential at the α -sites by decimating the side coupled QD. This leads to a *renormalized* value of the on-site potential at the α -vertex, given by, $\bar{\epsilon}_\alpha = \epsilon_0 + \lambda^2/(E - \epsilon_\mu)$.

The Schrödinger equation for the two-arm ladder can now be written equivalently in the form of the difference

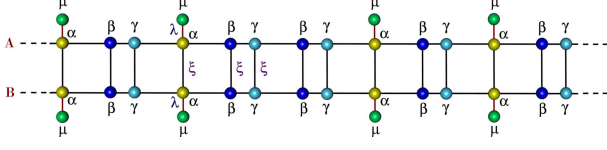


FIG. 1: (Color online) Typical realization of a two strand Fibonacci ladder. The sites α , β and γ are colored differently to distinguish between the nearest neighbor bond-environments. The adatoms μ are coupled to the α -sites in each case. The coupling between μ and α -site is denoted by λ and the inter-strand coupling is denoted by ξ .

equations involving 2×2 matrices:

$$(EI - \epsilon_i)\psi_i = \sum_j t_{ij}\psi_j \quad (2)$$

Written explicitly, the matrix equation reads,

$$\left[\begin{pmatrix} E & 0 \\ 0 & E \end{pmatrix} - \begin{pmatrix} \epsilon_i & \xi \\ \xi & \epsilon_i \end{pmatrix} \right] \begin{pmatrix} \psi_{i,A} \\ \psi_{i,B} \end{pmatrix} = \begin{pmatrix} t_{i,i+1}^A & 0 \\ 0 & t_{i,i+1}^B \end{pmatrix} \begin{pmatrix} \psi_{i+1,A} \\ \psi_{i+1,B} \end{pmatrix} + \begin{pmatrix} t_{i,i-1}^A & 0 \\ 0 & t_{i,i-1}^B \end{pmatrix} \begin{pmatrix} \psi_{i-1,A} \\ \psi_{i-1,B} \end{pmatrix} \quad (3)$$

In Eq. (3), the potential ϵ_i takes on values $\bar{\epsilon}_\alpha$ corresponding to a renormalized α -site in each arm, while it is equal to ϵ_0 for both the β and γ -sites in each arm. The nearest neighbor hopping integrals $t_{i,i\pm 1}^{A(B)}$ are t_L or t_S depending on the local environment of the corresponding site in the arm $A(B)$. A look at the Fig. 1 will make it obvious that there are three such equations corresponding to the three different kinds of vertices viz., α , β and γ respectively. The potential matrix corresponding to the renormalized α -sites is,

$$\begin{pmatrix} \epsilon_0 + \frac{\lambda^2}{E - \epsilon_\mu} & \xi \\ \xi & \epsilon_0 + \frac{\lambda^2}{E - \epsilon_\mu} \end{pmatrix} \equiv \epsilon_0 + \frac{\lambda^2}{E - \epsilon_\mu} \mathbf{I} \quad (4)$$

and that for the β and γ sites are

$$\epsilon_0 = \begin{pmatrix} \epsilon_0 & \xi \\ \xi & \epsilon_0 \end{pmatrix} \quad (5)$$

We now make a similarity transformation on the ϵ_0 -matrices using a matrix \mathbf{S} and change over to a new basis $\phi_i = \mathbf{S}^{-1}\psi_i$ [27]. This leads to a decoupling of the set of Eq. (3) into two independent sets, one corresponding to the A -arm alone, and the other, to the arm B . Each independent set corresponds to two different quasi-periodic Fibonacci chains. Written explicitly, the equations read,

$$\begin{aligned} \left[E - \left(\epsilon_0 + \xi + \frac{\lambda^2}{E - \epsilon_\mu} \right) \right] \phi_{i,A} &= t_L \phi_{i+1,A} + t_L \phi_{i-1,A} \\ [E - (\epsilon_0 + \xi)] \phi_{i,A} &= t_S \phi_{i+1,A} + t_L \phi_{i-1,A} \\ [E - (\epsilon_0 + \xi)] \phi_{i,A} &= t_L \phi_{i+1,A} + t_S \phi_{i-1,A} \end{aligned} \quad (6)$$

for the sites α , β and γ sequentially in arm A . Similar

set of equations for the arm B will be,

$$\begin{aligned} \left[E - \left(\epsilon_0 - \xi + \frac{\lambda^2}{E - \epsilon_\mu} \right) \right] \phi_{i,B} &= t_L \phi_{i+1,B} + t_L \phi_{i-1,B} \\ [E - (\epsilon_0 - \xi)] \phi_{i,B} &= t_S \phi_{i+1,B} + t_L \phi_{i-1,B} \\ [E - (\epsilon_0 - \xi)] \phi_{i,B} &= t_L \phi_{i+1,B} + t_S \phi_{i-1,B} \end{aligned} \quad (7)$$

Needless to say, each of the sets Eq. (6) and Eq. (7) separately represents an independent Fibonacci chain. The spectrum of each chain bears the usual singular continuous character. The spectrum of the original ladder network can be obtained by convolution of the density of states of the individual decoupled Fibonacci chains. However, an analysis of these decoupled subsystems yields rich spectral insight that would otherwise be difficult to obtain. We are now in a position to throw some light on this issue.

First, we need to appreciate that, in the new basis each decoupled Fibonacci chain is described by a set of three *transfer matrices*, viz., \mathbf{M}_α , \mathbf{M}_β and \mathbf{M}_γ [35]. For the A -arm Fibonacci chain, the explicit expressions of these matrices are,

$$\begin{aligned} \mathbf{M}_{\alpha,A} &= \begin{pmatrix} [E - (\epsilon_0 + \xi + \frac{\lambda^2}{E - \epsilon_\mu})]/t_L & -1 \\ 1 & 0 \end{pmatrix} \\ \mathbf{M}_{\beta,A} &= \begin{pmatrix} [E - (\epsilon_0 + \xi)]/t_S & -t_L/t_S \\ 1 & 0 \end{pmatrix} \\ \mathbf{M}_{\gamma,A} &= \begin{pmatrix} [E - (\epsilon_0 + \xi)]/t_L & -t_S/t_L \\ 1 & 0 \end{pmatrix} \end{aligned} \quad (8)$$

respectively.

A similar set of transfer matrices for the decoupled B -

arm reads,

$$\begin{aligned} M_{\alpha,B} &= \begin{pmatrix} [E - (\epsilon_0 - \xi - \frac{\lambda^2}{E - \epsilon_\mu})]/t_L & -1 \\ 1 & 0 \end{pmatrix} \\ M_{\beta,B} &= \begin{pmatrix} [E - (\epsilon_0 - \xi)]/t_S & -t_L/t_S \\ 1 & 0 \end{pmatrix} \\ M_{\gamma,B} &= \begin{pmatrix} [E - (\epsilon_0 + \xi)]/t_L & -t_S/t_L \\ 1 & 0 \end{pmatrix} \end{aligned} \quad (9)$$

M_α and $M_{\gamma\beta} = M_\gamma M_\beta$ follow an arrangement in the Fibonacci sequence [35].

Speaking in terms of the individual decoupled Fibonacci chains A and B , we already know that each such chain offers a singular continuous spectrum and, if $\lambda = 0$, transfer matrices exhibit a *six cycle* in each case at the energy values $E = \epsilon_0 \pm \xi$. The six cycle of the matrix map ensures that the said energy values belong to the spectrum of the infinite Fibonacci chain [35]. Thus, by decoupling we have obtained at least two eigenvalues which definitely belong to the spectrum of the infinite ladder. Extending this idea to an n -strand Fibonacci ladder we can easily identify n different energy eigenvalues of the full quasi 1-d Fibonacci network in the absence of λ (i.e. detaching the QD's) in a completely analytical way. The task becomes non-trivial when one consider the QPLN as a whole, without decoupling. Now let us see how one can generate a continuum in the spectrum of such a ladder network by incorporating the QD's (i.e. for $\lambda \neq 0$).

Let us choose Eq. (8). We set $\epsilon_\mu = \epsilon_0 + \xi$. It can easily be verified that, with this potential, the commutator $[M_\alpha, M_{\beta\gamma}] = 0$ for the decoupled A -arm, *irrespective of the energy E* of the electron, if $\lambda = \sqrt{t_S^2 - t_L^2}$. This implies that, with these conditions the individual α -vertices and the $\beta\gamma$ dimers in the decoupled A -arm can be arranged in any desired pattern, for example, in a perfectly periodic pattern. The spectrum offered by the decoupled A -arm Fibonacci chain will thus, under this choice of the QD potential ϵ_μ and the tunnel hopping λ , will turn out to be *indistinguishable* from that of a perfectly periodic sequence of the α -site (the 'renormalized' α -site, to be precise) and the $\beta\gamma$ doublet. Under such condition, the decoupled A -arm will contribute two *absolutely continuous* sub-bands to the full two-arm Fibonacci ladder.

It should be appreciated that once we fix $\epsilon_\mu = \epsilon_0 + \xi$, the set of Eq. (9) represents a mixed model linear Fibonacci chain. The energy spectrum is the usual fragmented, multi-fractal one. As the full spectrum of the two-arm ladder will be a convolution of both, we expect it to have absolutely continuous parts decorated with a spiky envelope, and a mixture of *extended* Bloch-like states and the *critical* eigenfunctions which are characteristic of a quasi-periodic Fibonacci sequence of potentials.

2. The RSRG analysis

The above arguments are confirmed by a real space renormalization group (RSRG) calculation of the local density of states of the full two-arm Fibonacci ladder (without decoupling it). To do this, we renormalize the full two-strand ladder by decimating the β -vertices. This generates *new* hopping integrals across the diagonals of the fundamental rectangular plaquettes of renormalized ladder denoted by d'_L and d'_S in the equations to follow. To implement the decimation we need to assign three different symbols to the inter-arm hopping ξ , viz., ξ_α , ξ_β and ξ_γ connecting the α , β and γ vertices of the two strands. Of course, we begin with $\xi_\alpha = \xi_\beta = \xi_\gamma = \xi$. The recursion relations arising out of this decimation procedure are given by,

$$\begin{aligned} \epsilon'_\alpha &= \epsilon_\gamma + \mathcal{A}t_L + \mathcal{B}t_S + \mathcal{C}d_L + \mathcal{D}d_S \\ \epsilon'_\beta &= \epsilon_\gamma + \mathcal{B}t_S + \mathcal{D}d_S \\ \epsilon'_\gamma &= \bar{\epsilon}_\alpha + \mathcal{A}t_L + \mathcal{C}d_L \\ t'_L &= \mathcal{B}t_L + \mathcal{D}d_L \\ t'_S &= t_L \\ d'_L &= \mathcal{B}d_L + \mathcal{D}t_L \\ d'_S &= d_L \\ \xi'_\alpha &= \xi_\gamma + \mathcal{A}d_L + \mathcal{B}d_S + \mathcal{C}t_L + \mathcal{D}t_S \\ \xi'_\beta &= \xi_\gamma + \mathcal{B}d_S + \mathcal{D}t_S \\ \xi'_\gamma &= \xi_\alpha + \mathcal{A}d_L + \mathcal{C}t_L \end{aligned} \quad (10)$$

where

$$\begin{aligned} \mathcal{A} &= \frac{(E - \epsilon_\beta)t_L + \xi_\beta d_L}{\mathcal{W}} \\ \mathcal{B} &= \frac{(E - \epsilon_\beta)t_S + \xi_\beta d_S}{\mathcal{W}} \\ \mathcal{C} &= \frac{(E - \epsilon_\beta)d_L + \xi_\beta t_L}{\mathcal{W}} \\ \mathcal{D} &= \frac{(E - \epsilon_\beta)d_S + \xi_\beta t_S}{\mathcal{W}} \\ \mathcal{W} &= (E - \epsilon_\beta)^2 - \xi_\beta^2 \\ \bar{\epsilon}_\alpha &= \epsilon_0 + \lambda^2/(E - \epsilon_\mu) \end{aligned}$$

The initial values of the diagonal hoppings d_L and d_S are of course set equal to zero as initially there is no diagonal hopping. It grows as a product of RSRG decimation scheme.

A small imaginary part is added to the energy E , and the LDOS at an α , β or γ site is obtained by calculating the respective local Green's function $G_{00}^i = (E - \epsilon_i^*)^{-1}$, where $i = \alpha, \beta$ or γ . ϵ_i^* represents the fixed point of the respective on-site potential as the hopping integrals flow to zero under the RSRG iterations. The LDOS is given by,

$$\rho_i = -\frac{1}{\pi} \text{Im}[G_{00}^i] \quad (11)$$

The results are presented in Fig. 2. In panel (a) the spectra of the decoupled A - and B -arms are shown separately, while panel (b) illustrates the spectrum of the full two-arm ladder as obtained from the RSRG study. The existence of the absolutely continuous portions in the energy spectrum is obvious. The character of the eigenfunctions belonging to the spectrum is checked from an observation of the flow of the hopping integrals t_L , t_S and the diagonal hopping amplitude under RSRG iterations. For any energy eigenvalue, chosen from any portion of the absolutely continuous sub-bands (grey shaded portion in Fig. 2(a)) all the hopping integrals remain non-zero for an arbitrarily large number of iterations confirming the extended character of the wave functions. Beyond the extended regime, the hopping integrals flow to zero under iteration indicating that the eigenfunctions are not extended. In Fig. 2(b) we see the full LDOS spectrum from the coupled two-strand QPLN. the eigenstates form a mixed spectrum of critical and extended states, though any evidence of phase transition or even a crossover is not proved.

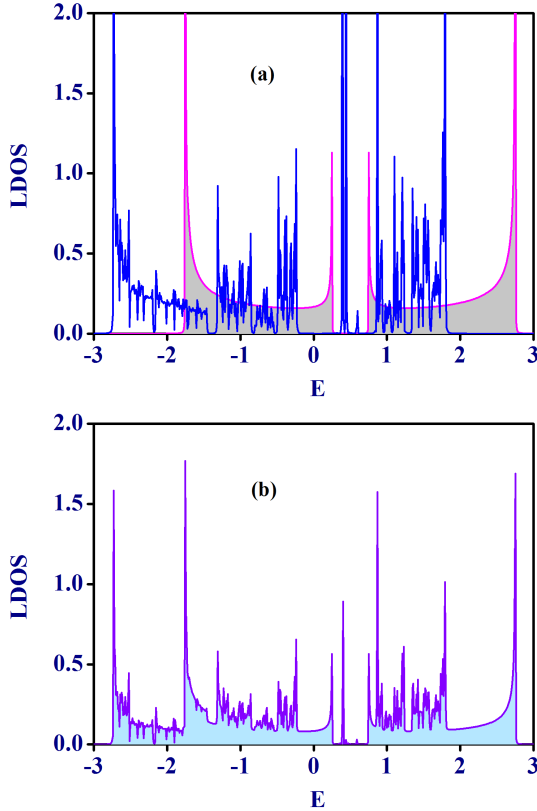


FIG. 2: (Color online) Plot of local density of states (LDOS) at an α -vertex for a two-strand ladder network. The upper panel shows the LDOS spectra of the decoupled individual linear chains, one chain satisfying resonance condition. The lower panel shows the LDOS spectrum of the composite ladder network as obtained from the RSRG scheme, under resonance condition. The values of the parameters chosen are $\epsilon_\alpha = \epsilon_\beta = \epsilon_\gamma = 0$, $\epsilon_\mu = 0.5$, $t_L = 1$, $t_S = 1.25$, $\lambda = 0.75$, and $\xi = 0.5$, measured in unit of t_L .

An additional support in regard of the continuous sub-bands and the extended eigenstates is also obtained from an observation of the flow pattern of the entire parameter space of the decoupled strand that satisfies the condition $\epsilon_\mu = \epsilon_0 + \xi$ and $\lambda = \sqrt{t_L^2 - t_S^2}$. For such a choice, under successive RSRG step, we always get $\tilde{\epsilon}_\alpha^{(j)} \neq \epsilon_\beta^{(j)} = \epsilon_\gamma^{(j)}$ and $t_L^{(j)} \neq t_S^{(j)}$. This confirms the extended Bloch-like character of the wave function for the entire energy regime (given by the grey color in Fig. 2(a)) as discussed elsewhere [36].

B. Three-arm Fibonacci ladder and beyond

The motivation behind extending the above analysis to a three-arm Fibonacci ladder stems from the curiosity

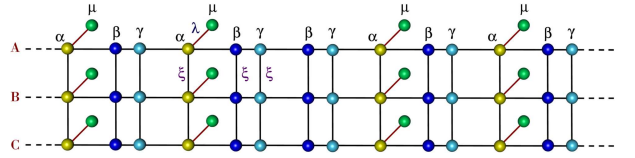


FIG. 3: (Color online) Schematic diagram of a three-strand Fibonacci ladder network. Meaning of all other symbols are same as in Figure 1.

to know whether, as one extends the ladder network in the transverse direction, any possibility of a re-entrant transition (or, crossover) from a singular continuous to an absolutely continuous energy spectrum becomes apparent. For disordered ladders comprising the same α and $\beta\gamma$ clusters this would imply the possibility of an *insulator-metal* transition that can be triggered by an appropriate choice of the numerical values of the QD potential ϵ_μ and the tunnel hopping integral λ .

To check such a possibility we decouple a three-arm Fibonacci ladder (Fig. 3). We follow the same prescription for decoupling as outlined in the case of a two-strand ladder. Diagonalization of the potential matrix ϵ_i now yields three eigenvalues, viz., ϵ_0 and $\epsilon_0 \pm \sqrt{2}\xi$, and the effective potential at the α -site in each decoupled arm will be $\epsilon_0 + \lambda^2/(E - \epsilon_\mu)$ (for arm A , say), $\epsilon_0 + \sqrt{2}\xi + \lambda^2/(E - \epsilon_\mu)$ (for arm B , say) and $\epsilon_0 - \sqrt{2}\xi + \lambda^2/(E - \epsilon_\mu)$ (for arm C). We now end up having three sets of equations, one for each decoupled strand. For example,

$$\begin{aligned} \left[E - \left(\epsilon_0 + \frac{\lambda^2}{E - \epsilon_\mu} \right) \right] \phi_{i,A} &= t_L \phi_{i+1,A} + t_L \phi_{i-1,A} \\ (E - \epsilon_0) \phi_{i,A} &= t_S \phi_{i+1,A} + t_L \phi_{i-1,A} \\ (E - \epsilon_0) \phi_{i,A} &= t_L \phi_{i+1,A} + t_S \phi_{i-1,A} \end{aligned} \quad (12)$$

corresponding to the α , β and γ sites respectively in the decoupled A -strand. Two sets of similar equations are also obtained for the decoupled B - and C -strands, with the effective potential at the α -site being equal to $\epsilon_0 + \sqrt{2}\xi + \lambda^2/(E - \epsilon_\mu)$ and $\epsilon_0 - \sqrt{2}\xi + \lambda^2/(E - \epsilon_\mu)$ respectively.

The effective potentials at the β and γ sites in the B and C strand are $\epsilon_0 \pm \sqrt{2}\xi$ as there is no side coupling to these sites.

If, as before, we set $\epsilon_\mu = \epsilon_0$ in Eq. (12), then $[M_\alpha, M_{\beta\gamma}] = 0$ for the decoupled A -strand. The contribution to the full spectrum coming from this separate chain will be two absolutely continuous sub-bands. With the potential of the QD set at $\epsilon_\mu = \epsilon_0$, the two other decoupled strands represent two different Fibonacci chains in the mixed model. The spectrum resulting from each of them will remain fragmented Cantor type. The overall spectrum, as we now have known, will be a convolution of the three. The absolutely continuous portions will still hold their positions in the main spectrum, and will be flanked by the spiky, fragmented parts characteristics of critical eigenstates of a Fibonacci lattice (Fig 4). The eigenfunctions belonging to the continuous sub-bands will, needless to say, be of extended character.

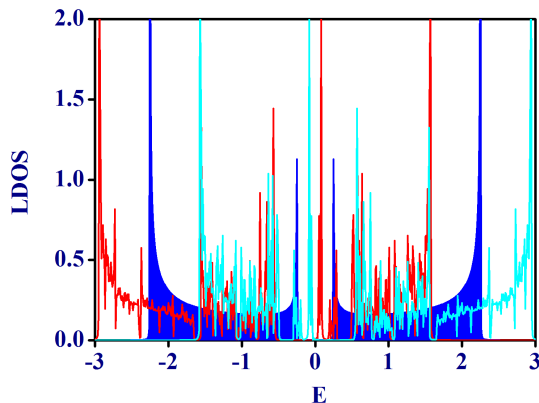


FIG. 4: (Color online) Plot of LDOS for a three-strand Fibonacci ladder network. It represents the LDOS spectra of the three decoupled isolated chains, one satisfying resonance condition (in blue shaded color) and the other two with off-resonance condition (in red and cyan color). The parameters chosen here are same as in Figure 2.

One needs to appreciate that each spectrum offered separately by the decoupled B - and C -strands will have different “band-centres” around which the singular continuous spectra of the individual decoupled Fibonacci chain will spread out. With an n -strand ladder model, there will be $n - 1$ such centers from the $n - 1$ decoupled strands around which Cantor set energy eigenvalues will be distributed, the remaining strand contributing the absolutely continuous sub-bands. The centres will be densely populated around the outer edge of the continuous sub-bands as $n \rightarrow \infty$. Thus, with increasing number of strands there is a possibility of observing a smooth critical to extended state crossover in the spectrum of such quasi 1-d aperiodic ladder models. Clearly, the argument prevails even if we have an n -strand off diagonally disordered ladder network. The side coupled QD’s with appropriately tuned potential one can then expect a re-entrant *insulator-metal* transition.

III. TWO TERMINAL TRANSMISSION

Above results are corroborated by detailed calculation of the two terminal transmission coefficient. The central idea has already been elaborated in the existing literature [37]. The ladder is clamped between two semi-infinite perfectly ordered leads (viz., the source and the drain) at any two extremities (Fig. 5). The portion of the

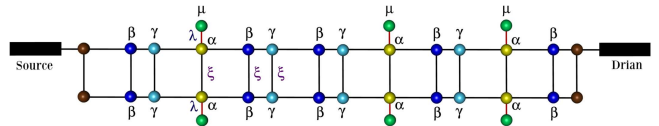


FIG. 5: (Color online) Schematic view of a finite size two-strand QPLN clamped between the source and the drain. The extreme left and the extreme right sites are colored differently compared to the bulk sites to signify that they have different status as compared to those in the bulk of the lattice.

ladder is then sequentially decimated to bring it down to a *diatomic molecule*, and the transmission coefficient is easily obtained [38]. To save space, we do not provide the details. Only one result is shown in which the two semi-infinite ordered leads are connected to the extreme points of the upper strand of a 12-th generation Fibonacci ladder. The existence of the continuous parts in the en-

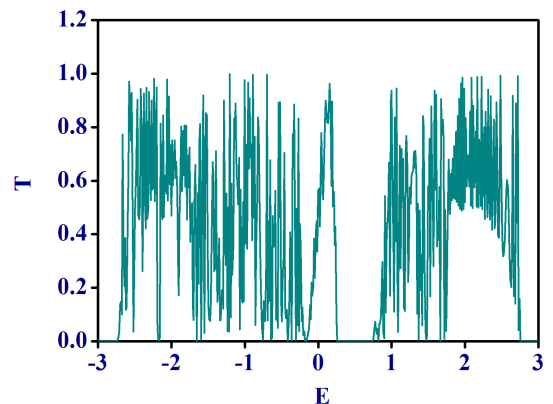


FIG. 6: (Color online) Transmission characteristics of a 12-th generation two-strand Fibonacci ladder network under resonance condition. Both the incoming and outgoing leads, viz., the source and the drain are connected in the upper strand. System parameters chosen are $\epsilon_\alpha = \epsilon_\beta = \epsilon_\gamma = 0$, $\epsilon_\mu = 0.5$, $t_L = 1$, $t_S = 1.25$, $\lambda = 0.75$, and $\xi = 0.5$, and the lead parameters are $\epsilon_L = 0$ and $\tau_L = 2$.

ergy spectrum of the infinite system is already showing up in the enhanced value of the transmission coefficient at appropriate values of the electron energy (Fig. 6).

IV. CONCLUDING REMARKS

We have shown that Fibonacci quasi-periodic ladder networks, where quasi-periodic order is introduced in the

distribution of bonds, keeping the potential at every vertex same, are capable of producing absolutely continuous portions in their energy spectra. This requires the attachment of quantum dots from one side to a special set of sites in each arm of the ladder. A suitable adjustment of the dot potential, together with the dot-backbone coupling can generate absolutely continuous energy subbands, decorated at the flanks by the usual critical states – a characteristics of quasi-periodic lattices. Apart from opening up the possibility of engineering the transport of excitons in such multi-strand systems, a very basic issue of Anderson localization is reviewed. It seems that, the existence of localized eigenstates in similar disordered ladder networks may strongly depend on the numerical

values of the parameters in the Hamiltonian.

The analysis is carried over to other quasi-periodically ordered systems, such as the copper mean chain, where the condition becomes much more non-trivial. These issues will be reported in a forthcoming article.

Acknowledgments

B.P. is grateful to DST, India for an INSPIRE Fellowship. A.C. acknowledges financial support from DST, India through a PURSE grant.

-
- [1] P. W. Anderson, Phys. Rev. **109**, 1492 (1958).
 - [2] B. Kramer and A. MacKinnon, Rep. Prog. Phys. **56**, 1469 (1993).
 - [3] E. Abrahams, P. W. Anderson, D. C. Liciardello, and T. V. Ramakrishnan, Phys. Rev. Lett. **42**, 673 (1979).
 - [4] E. Yablonovitch, Phys. Rev. Lett. **58**, 2059 (1987).
 - [5] S. John, Phys. Rev. Lett. **58**, 2486 (1987).
 - [6] F. R. Montero de Espinosa, E. Jiménez, and M. Torres, Phys. Rev. Lett. **80**, 1208 (1998).
 - [7] J. O. Vasseur, P. A. Deymier, G. Frantziskonis, G. Hong, B. Djafari-Rouhani, and L. Dobrzynski, J. Phys.: Condens. Matter **10**, 6051 (1998).
 - [8] I. O. Barinov, A. P. Alodzhants, and S. M. Arakelyan, Quantum Electron. **39**, 685 (2009).
 - [9] M. Grochol and C. Piermarocchi, Phys. Rev. B **78**, 035323 (2008).
 - [10] A. Tao, P. Sinsermsuksaul, and P. Yang, Nature Nanotechnol. **2**, 435 (2007).
 - [11] A. Christ, Y. Ekinci, H. H. Solak, N. A. Gippus, S. G. Tikhodeev, and O. J. F. Martin, Phys. Rev. B **76**, 201405 (2007).
 - [12] B. Damski *et al.*, Phys. Rev. Lett. **91**, 080403 (2003).
 - [13] J. Billy *et al.*, Nature (London) **453**, 891 (2008).
 - [14] G. Roati *et al.*, Nature (London) **453**, 895 (2008).
 - [15] R. A. Römer and H. Schulz-Baldes, Europhys. Lett. **68**, 247 (2004).
 - [16] A. Eilmes, R. A. Römer, and M. Schreiber, Physica B **296**, 46 (2001).
 - [17] A. Rodríguez, J. Phys. A: Math. Gen. **39**, 14303 (2006).
 - [18] A. Rodríguez, L. J. Vasquez, and R. A. Römer, Phys. Rev. B **78**, 195107 (2008).
 - [19] A. Rodríguez, L. J. Vasquez, K. Slevin, and R. A. Römer, Phys. Rev. B **84**, 134209 (2011).
 - [20] S. D. Pinski, W. Schirmacher, and R. A. Römer, Europhys. Lett. **97**, 16007 (2012).
 - [21] Lev I. Deych, A. A. Lisyanski, and B. L. Alshuler, Phys. Rev. Lett. **84**, 2678 (2000).
 - [22] M. Titov and H. Schomerus, Phys. Rev. Lett. **95**, 126603 (2005).
 - [23] J. W. Kantelhardt and A. Bunde, Phys. Rev. B **66**, 035118 (2002).
 - [24] P. Mohanty and R. A. Webb, Phys. Rev. Lett. **88**, 146601 (2002).
 - [25] D. H. Dunlap, H.-L. Wu, and P. Phillips, Phys. Rev. Lett. **65**, 88 (1990).
 - [26] F. A. B. F. de Moura and M. Lyra, Phys. Rev. Lett. **81**, 3735 (1998).
 - [27] S. Sil, S. K. Maiti, and A. Chakrabarti, Phys. Rev. B **78**, 113103 (2008).
 - [28] A. Rodriguez, A. Chakrabarti, and R. A. Römer, Phys. Rev. B **86**, 085119 (2012).
 - [29] A. Chakrabarti, S. N. Karmakar, and R. K. Moitra, Phys. Rev. B **50**, 13276 (1994).
 - [30] E. Maciá, Phys. Rev. B **74**, 245105 (2006); Phys. Rev. B **80**, 125102 (2009).
 - [31] M. Bravi, R. Farchioni, G. Grosso, and G. P. Parravicini, Phys. Rev. B **87**, 035105 (2013).
 - [32] R. Farchioni, G. Grosso, and G. P. Parravicini, Eur. Phys. J. B **84**, 227 (2011).
 - [33] B. Kubala and J. König, Phys. Rev. B **67**, 205303 (2003).
 - [34] R. Farchioni, G. Grosso, and G. P. Parravicini, Phys. Rev. B **85**, 165115 (2012).
 - [35] M. Kohmoto, B. Sutherland, and C. Tang, Phys. Rev. B **35**, 1020 (1987).
 - [36] B. Pal, S. K. Maiti, and A. Chakrabarti, Europhys. Lett. **102**, 17004 (2013).
 - [37] A. D. Stone, J. D. Joannopoulos, and D. J. Chadi, Phys. Rev. B **24**, 5583 (1981).
 - [38] B. Pal and A. Chakrabarti, Eur. Phys. J. B **85**, 307 (2012).